

# Synthesis and characterization of fluorescent graft fluorene-co-polyphenol derivatives: The effect of substituent on solubility, thermal stability, conductivity, optical and electrochemical properties

İsmet Kaya\*, Mehmet Yıldırım, Aysel Aydın, Dilek Şenol

Çanakkale Onsekiz Mart University, Faculty of Sciences and Arts, Department of Chemistry, 17020 Çanakkale, Turkey

## ARTICLE INFO

### Article history:

Received 26 February 2010  
Received in revised form 12 July 2010  
Accepted 13 July 2010  
Available online 21 July 2010

### Keywords:

Graft copolymer  
Oligophenol  
Fluorescence  
Conjugated polymers  
Polyfluorene

## ABSTRACT

A series of fluorene Schiff bases and their oligophenol derivatives were successfully synthesized using the condensation and graft copolymerization reactions, respectively. The synthesized compounds were good soluble in common organic solvents. Photoluminescence (PL) properties of the synthesized materials were determined in solution forms. As to the fluorene copolymers (FPs), higher PL intensities were obtained when compared with the monomeric models. Solvent effects on the fluorescence spectra and possible usages in spectrofluorometric ion sensors of the FPs were discussed. Optical and electrochemical band gaps of the polymers were lower than those of the Schiff bases indicating the more conjugated structures of the FPs. The oxidized states of the novel fluorene compounds were also examined by cyclic voltammetry (CV) technique. The solid state conductivity measurements showed that the synthesized FPs were semiconductors and when exposed to the iodine vapour their conductivities could be increased up to four orders of magnitude. The polymer having the lower band gap (FP-3) had also the highest undoped conductivity. Thermal characterizations of the synthesized compounds were carried out by TG-DTA and DSC methods. The initial degradation temperatures of the FPs were found quite high in the range of 220–300 °C.

© 2010 Elsevier Ltd. All rights reserved.

## 1. Introduction

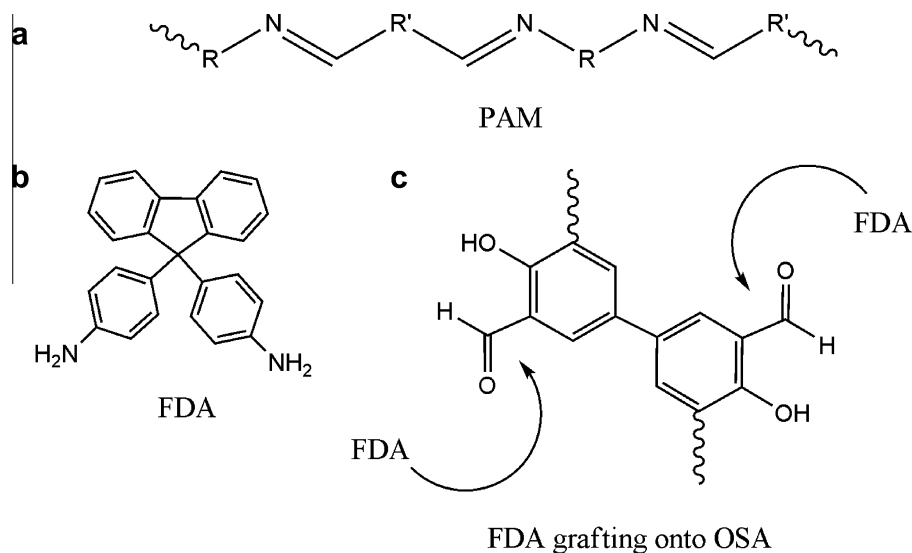
Polyfluorenes (PFs) and their derivatives have attracted much attention of researchers due to their interesting properties like high luminescence efficiency, thermal stability, and low band gaps [1–4]. Different methods have been reported for preparing of PFs such as oxidative polymerization in presence of  $\text{FeCl}_3$  [5,6], electro polymerization [7,8] and transition-metal-catalyzed reactions (Yamamoto's and Suzuki's coupling reactions) [9]. Fukuda et al. reported the first soluble PFs at the end of 1980s using  $\text{FeCl}_3$ -catalyzed oxidative coupling polymerization reaction [9]. However, the first regio-regular synthesis of PFs were accomplished by nickel-catalyzed Yamamoto coupling and palladium-catalyzed Suzuki coupling reactions of 2,7-dibromofluorene and 2,7-diboronylfluorene derivatives [10]. Nowadays, both methods represent the most important routes to obtain the PFs. The another methodology occasionally used is Stille coupling [11].

Fluorene moiety was also used in synthesizing of polyazomethines as hole-facilitating unit. Soluble kinds of azomethine copolymers of 9,9'-bis(4-aminophenyl)fluorene (FDA) were obtained by

the condensation reaction of FDA with aromatic dialdehydes containing carbazole or thiophene units [12]. The obtained polymers were observed to have both fine thermal stability and high solubility in common organic solvents. Bruma et al. reported FDA co-polyazomethines as blue light emitting polymers with the oxadiazole rings as the side groups [13]. Polyamide derivatives of FDA were investigated with their photoluminescence, electrochemical, optical, and thermal properties [14] and quite high-thermal-stability and luminescence efficiency were recorded. Co-polyazomethine derivatives of 2,7-diaminofluorene were also synthesized with dodecyl-substituted 2,5-diformylthiophene [15] and 2,5-diformyl-3-hexylthiophene [16]. However, in all mentioned studies fluorene moiety was in successive co-polymer structures. In the present study we proposed graft co-polyazomethine derivatives of FDA with oligophenol structures and investigated the effects of fluorene moiety as a side chain. A typical structure of a basic polyazomethine (PAM), FDA, and the graft copolymerization of FDA were shown in Scheme 1.

Schiff base substituted oligophenol derivatives were studied by Kaya et al. with their useful properties including optical, electrochemical, electrical, and thermal characteristics [17–22]. This class of oligophenols is generally synthesized by oxidative polycondensation reaction (OP) of the corresponding Schiff base using cheap

\* Corresponding author. Tel.: +90 286 218 00 18; fax: +90 286 218 05 33.  
E-mail address: [kayaismet@hotmail.com](mailto:kayaismet@hotmail.com) (İ. Kaya).



**Scheme 1.** The structures of a typical PAM, FDA, and graft copolymerization of FDA.

oxidants like NaOCl, H<sub>2</sub>O<sub>2</sub>, and air. The OP reaction was monitored by examining the growth of new absorption peaks over time [23]. The electrical conductivity of the azomethine bonds in these kinds of polymers can be increased by doping with iodine [24]. Graft copolyphenol derivatives of polyazomethines were also synthesized using melamine as the grafting agent [25]. Melamine co-polyphenol derivatives were found as thermally stable and semi-conductive after a long time doping with iodine.

In this study we aimed to combine the advantages of the fluorene moiety and oligophenol based polyazomethines. For this purpose we grafted FDA units onto aromatic oligohydroxy aldehydes (OSA, O-4-HBA, and O-3,4-HBA) by azomethine linkages which resulted in the polyconjugated fluorene polymers. The Schiff base models of FDA were also prepared by condensation reaction with salicylaldehyde, 4-hydroxybenzaldehyde, and 3,4-dihydroxybenzaldehyde. Characterization was made by UV-vis, FT-IR, NMR, and SEC analyses. Fluorescence characteristics were determined in five different solvents and a blue light emission for the presented fluorene polymers was obtained as in the literature [13]. Electrical conductivities, electrochemical analyses, and the thermal characteristics were also investigated.

## 2. Experimental

### 2.1. Materials

9,9'-bis(4-aminophenyl)fluorene (FDA), salicylaldehyde, 4-hydroxybenzaldehyde, 3,4-dihydroxybenzaldehyde, dimethylformamide (DMF), dimethylsulfoxide (DMSO), tetrahydrofuran (THF), dioxane, methanol, ethanol, acetonitrile, acetone, toluene, ethyl acetate, heptane, hexane, CCl<sub>4</sub>, CHCl<sub>3</sub>, H<sub>2</sub>SO<sub>4</sub>, KOH and HCl were supplied from Merck Chemical Co. (Germany) and they were used as received. 30% aqueous solution of sodium hypo chloride, NaOCl was supplied by Paksoy Chemical Co. (Turkey).

### 2.2. Syntheses of the fluorene Schiff bases

Fluorene Schiff bases abbreviated as FM-1, FM-2, and FM-3 were synthesized by the condensation reaction of FDA with salicylaldehyde, 4-hydroxybenzaldehyde, and 3,4-dihydroxybenzaldehyde, respectively. Reactions were performed as follows: FDA

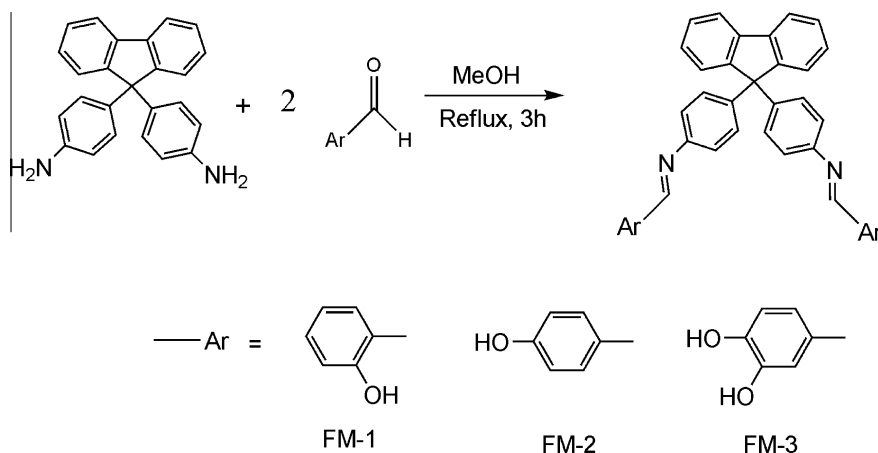
(1.740 g, 0.005 mol) was placed into a 250 ml three-necked round-bottom flask which was fitted with condenser, thermometer and magnetic stirrer. Fifty milliliters of methanol was added into the flask and reaction mixture was heated up to 60 °C. A solution of salicylaldehyde (1.83 g, 0.015 mol), 4-hydroxybenzaldehyde (1.83 g, 0.015 mol), or 3,4-dihydroxybenzaldehyde (2.07 g, 0.015 mol) in 20 ml methanol was added into the flask. Reactions were maintained for 3 h under reflux (Scheme 2). The precipitated monomers was filtered, recrystallized from acetonitrile and dried in a vacuum desiccator. (yields: 85%, 74%, and 81% for FM-1, FM-2, and FM-3, respectively).

### 2.3. Syntheses of the FPs

Oligosalicylaldehyde (OSA), oligo-4-hydroxybenzaldehyde (O-4-HBA), and oligo-3,4-dihydroxybenzaldehyde (O-3,4-HBA) were synthesized by oxidative polymerization reaction of the corresponding monomers (salicylaldehyde, 4-hydroxybenzaldehyde, and 3,4-dihydroxybenzaldehyde, respectively) in an aqueous alkaline medium using NaOCl oxidant, as in the literature [26]. At the second step the fluorene co-polyphenols (FPs), FP-1, FP-2, and FP-3, were synthesized by grafting of FDA onto OSA, O-4-HBA, and O-3,4-HBA, respectively [25]. Reactions were made as follows: FDA (0.044 g, 0.003 mol) was placed into a 250 ml three-necked round-bottom flask which was fitted with condenser, thermometer and magnetic stirrer. 50 ml THF was added into the flask. Reaction mixture was heated up to 60 °C. OSA, O-4-HBA, and O-3,4-HBA (1.200 g, containing nearly 0.01 mol aldehyde groups) was separately solved in 20 ml THF and added into the flask. Reactions were maintained under reflux for 5 h and the reaction mixtures were cooled at the room temperature followed by evaporating in a vacuum evaporator (Scheme 3). The obtained products were washed with methanol and toluene (3 × 10 ml for each polymer) to separate from the unreacted FDA. Then, they were dried in a vacuum desiccator (yields: 57%, 62%, and 75% for FP-1, FP-2, and FP-3, respectively).

### 2.4. Characterization techniques

The solubility tests were done in different solvents by using 1 mg sample and 1 ml solvent at 25 °C. The infrared and ultraviolet-visible spectra were measured by Perkin Elmer FT-IR Spec-



Scheme 2. Syntheses of the monomers.

trum one and Perkin Elmer Lambda 25, respectively. The FT-IR spectra were recorded using universal ATR sampling accessory ( $4000\text{--}550\text{ cm}^{-1}$ ).  $^1\text{H}$  and  $^{13}\text{C}$  NMR spectra (Bruker AC FT-NMR spectrometer operating at 400 and 100.6 MHz, respectively) were also recorded by using deuterated DMSO- $d_6$  as a solvent at  $25\text{ }^\circ\text{C}$ . The tetramethylsilane was used as internal standard. Thermal data were obtained by using a Perkin Elmer Diamond Thermal Analysis system. TG-DTA measurements were made between 20 and  $1000\text{ }^\circ\text{C}$  (in  $\text{N}_2$ , rate  $10\text{ }^\circ\text{C}/\text{min}$ ). DSC analyses were carried out by using Perkin Elmer Pyris Sapphire DSC. DSC measurements were made between 25 and  $420\text{ }^\circ\text{C}$  (in  $\text{N}_2$ , rate  $20\text{ }^\circ\text{C}/\text{min}$ ). The number-average molecular weight ( $M_n$ ), weight average molecular weight ( $M_w$ ) and polydispersity index (PDI) were determined by size exclusion chromatography (SEC) techniques of Shimadzu Co. For SEC investigations a SGX (100 Å and 7 nm diameter loading material) 3.3 mm i.d.  $\times$  300 mm column was used; eluent: DMF (0.4 ml/min), polystyrene standards. A refractive index detector (RID) and UV detector were used to analyze the products at  $25\text{ }^\circ\text{C}$ .

### 2.5. Optical and electrochemical properties

Ultraviolet–visible (UV–vis) spectra were measured by Perkin Elmer Lambda 25. The absorption spectra were recorded by using DMSO at  $25\text{ }^\circ\text{C}$ . The optical band gaps ( $E_g$ ) were calculated from their absorption edges. Cyclic voltammetry (CV) measurements were carried out with a CHI 660 C Electrochemical Analyzer (CH Instruments, Texas, USA) at a potential scan rate of  $20\text{ mV}/\text{s}$ . All the experiments were performed in a dry box filled with argon at room temperature. The electrochemical potential of Ag was calibrated with respect to the ferrocene/ferrocenium ( $\text{Fc}/\text{Fc}^+$ ) couple. The half-wave potential ( $E^{1/2}$ ) of ( $\text{Fc}/\text{Fc}^+$ ) measured in acetonitrile solution of  $0.1\text{ M}$  tetrabutylammonium hexafluorophosphate ( $\text{TBAPF}_6$ ) was found to be  $0.39\text{ V}$  with respect to Ag wire. The voltammetric measurements were carried out in acetonitrile for the Schiff bases and acetonitrile/DMSO mixture (v/v: 10/1) for the polymers. The HOMO–LUMO energy levels and electrochemical band gaps ( $E_g'$ ) were calculated from the oxidation and reduction onset values [23].

### 2.6. Electrical properties

Polymer films were prepared on indium–tin–oxide (ITO) glass plates by dip-coating technique using a KSV Dip Coater instru-

ment. The process has been carried out by successive dipping and withdrawal of ITO glass plates in homogenous solutions of FP-1, FP-2, and FP-3 in THF (50 mg/ml for each solution) for 250 times. After each dipping the films were kept for 1 min for drying [27].

Conductivities of the synthesized polymers were measured on a Keithley 2400 Electrometer, using four point probe technique. Instrument was calibrated with ITO glass plate. Iodine doping was carried out by exposure of the polymer films to iodine vapour at atmospheric pressure in a desiccator at  $25\text{ }^\circ\text{C}$  [19,25]. Absorption spectra of the polymer films were measured before and after iodine doping by “Analytikjena Specord S 600” single beam spectrophotometer.

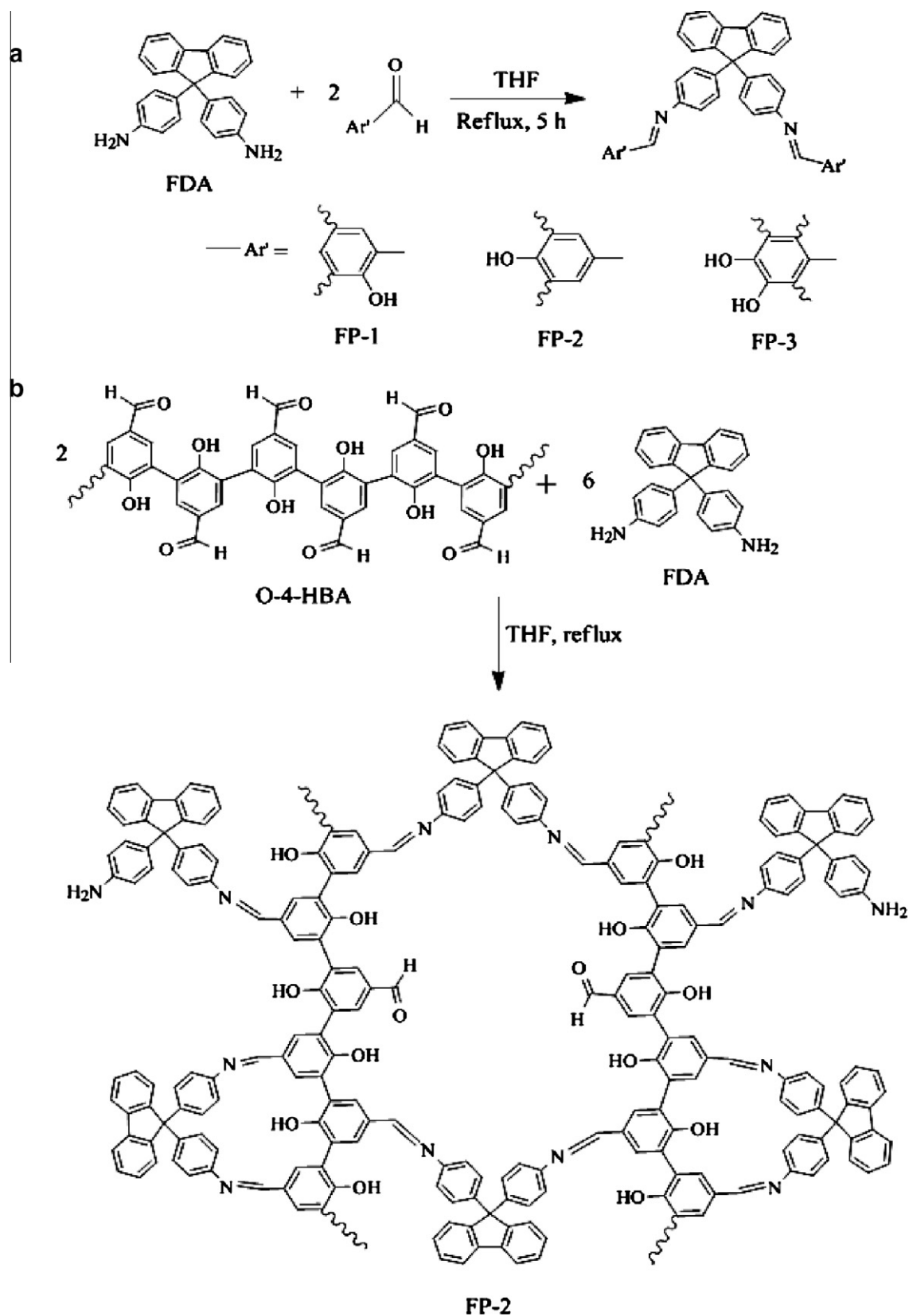
### 2.7. Fluorescence measurements

A Shimadzu RF-5301PC spectrofluorophotometer was used in fluorescence measurements. Emission and excitation spectra of the synthesized compounds were obtained in different solvents with the concentration of  $0.01\text{ mg}/\text{ml}$ . The optimum emission and excitation wavelengths in each solvent were determined. Also, optimizations of the concentrations to obtain maximal emission intensity values were investigated in DMF (for FM-1, FM-2, FP-2, and FP-3) and acetonitrile (for FM-3 and FP-1).

## 3. Results and discussion

### 3.1. Solubilities and structures of the compounds

The synthesized fluorene Schiff bases have light color-powder forms whereas their co-polyphenol derivatives are dark colored. The solubility test results are shown in Table 1. According to Table 1, FM-2 and FM-3 are fine soluble monomers in many employed solvents with exception some apolar solvents like benzene and *n*-hexane. However, their graft copolymers (FP-2 and FP-3) are only soluble in highly polar solvents like DMSO, DMF, and  $\text{H}_2\text{SO}_4$ . Whereas FM-1 is insoluble in methanol, ethylacetate and apolar solvents like benzene, dioxane, and *n*-hexane, it is completely soluble in chloroform, DMSO, DMF, and  $\text{H}_2\text{SO}_4$ . In addition, FP-1 is partially soluble in methanol, ethylacetate, benzene, and dioxane as different from FM-1.



The FT-IR spectra of the synthesized compounds are obtained. In all spectra a new peak appears in the range of 1608–1618  $\text{cm}^{-1}$  indicating the imine bond formation (HC=N stretch

vibration). The characteristic  $-\text{NH}_2$  and C=O stretch vibrations of FDA and the aromatic aldehydes disappear after the condensation reactions confirming the Schiff bases' structures. However, the FPs'

**Table 1**  
Solubility test results of the synthesized compounds.

Solvents	FM-1	FM-2	FM-3	FP-1	FP-2	FP-3
DMSO	+	+	+	+	+	+
Methanol	–	+	+	⊥	⊥	–
THF	+	+	+	+	⊥	⊥
Ethylacetate	–	+	+	⊥	–	–
DMF	+	+	+	+	+	+
H <sub>2</sub> SO <sub>4</sub>	+	+	+	+	+	+
CH <sub>3</sub> CN	⊥	+	+	⊥	–	–
Toluene	⊥	+	+	⊥	–	–
Benzene	–	–	–	⊥	–	–
1,4-Dioxane	–	+	+	⊥	–	–
n-Hexane	–	–	–	–	–	–
Chloroform	+	+	+	⊥	–	–

+: Soluble, ⊥: partially soluble, –: insoluble.

**Table 2**  
NMR analyses data of the synthesized compounds.

Compounds	Spectral data (δ ppm)
FM-1	<sup>1</sup> H NMR (DMSO): 13.05 (s, –OH), 9.02 (s, –CH=N–), 7.97 (d, –Hk), 7.62 (d, –Hd), 7.50 (d, –Hg), 7.42 (t, –Hj), 7.38 (t, –Hi), 7.33 (d, –Hf), 7.22 (d, –He), 6.97 (m, –Ha, –Hc) <sup>13</sup> C NMR (DMSO): 163.91 (C1- <i>ipso</i> ), 160.73 (C7–H), 150.78 (C8- <i>ipso</i> ), 147.25 (C11- <i>ipso</i> ), 144.65 (C13- <i>ipso</i> ), 140.02 (C18- <i>ipso</i> ), 133.77 (C3–H), 133.00 (C5–H), 129.18 (C10–H), 128.45 (C14,C15–H), 126.47 (C16,C17–H), 121.91 (C9–H), 121.18 (C4–H), 119.61 (C6- <i>ipso</i> ), 117.06 (C2–H), 64.87 (C12- <i>ipso</i> )
FM-2	<sup>1</sup> H NMR (DMSO): 10.29 (s, –OH), 8.41 (s, –CH=N–), 7.88 (d, –Hi), 7.78 (d, –Hb), 7.49 (d, –He), 7.36 (m, –Hf, –Hg), 7.18 (d, –Hd), 7.12 (d, –Hc), 6.92 (d, –Ha). <sup>13</sup> C NMR (DMSO): 163.86 (C1- <i>ipso</i> ), 160.38 (C5–H), 151.06 (C6- <i>ipso</i> ), 148.00 (C9- <i>ipso</i> ), 143.11 (C11- <i>ipso</i> ), 139.89 (C16- <i>ipso</i> ), 132.62 (C3–H), 131.17 (C8–H), 128.80 (C4- <i>ipso</i> ), 128.15 (C12–H), 127.99 (C13–H), 121.35 (C14–H), 120.82 (C15–H), 116.37 (C7–H), 114.22 (C2–H), 64.80 (C10- <i>ipso</i> )
FM-3	<sup>1</sup> H NMR (DMSO): 9.61 (s, –OH), 8.36 (s, –CH=N–), 7.88 (d, –Hj), 7.48 (d, Hf), 7.42 (t, –Hi), 7.31 (d, –Ha), 7.16 (s, –Hc), 6.94 (d, –He), 6.86 (t, –Hg), 6.77 (d, –Hb), 6.49 (d, –Hd) <sup>13</sup> C NMR (DMSO): 160.58 (C7–H), 152.66 (C3- <i>ipso</i> ), 152.00 (C8- <i>ipso</i> ), 146.16 (C4,C11- <i>ipso</i> ), 143.04 (C13- <i>ipso</i> ), 140.00 (C18- <i>ipso</i> ), 132.97 (C6- <i>ipso</i> ), 129.37 (C10–H), 128.93 (C14–H), 128.16 (C15–H), 126.44 (C16–H), 125.09 (C17–H), 122.97 (C1–H), 121.34 (C9–H), 116.04 (C2–H), 114.62 (C5–H), 64.44 (C12- <i>ipso</i> )
FP-1	<sup>1</sup> H NMR (DMSO): 12.99 (s, –OH), 8.91 (s, –CH=N–), 7.86–6.40 (m, aromatic), 5.00 (s, –NH <sub>2</sub> ). <sup>13</sup> C NMR (DMSO): 175.24 (s, –CH=O), 159.25 (C1- <i>ipso</i> ), 153.00 (C7–H), 148.50 (C8- <i>ipso</i> ), 145.23 (C11- <i>ipso</i> ), 140.29 (C13,C18- <i>ipso</i> ), 133.72 (C3,C4- <i>ipso</i> ), 130.01 (C10–H), 129.30 (C14–H), 128.27 (C15–H), 127.75 (C5–H), 126.70 (C16–H), 126.24 (C2- <i>ipso</i> ,C17–H), 121.25 (C9–H), 114.69 (C6- <i>ipso</i> ), 64.25 (C12- <i>ipso</i> )
FP-2	<sup>1</sup> H NMR (DMSO): 10.23 (s, –OH), 9.79 (s, –CH=O), 8.43 (s, –CH=N–), 7.86 (d, –Hg), 7.77 (d, –Hd), 7.35 (t, Hf), 7.28 (t, –He), 6.93 (d, –Ha), 6.81 (d, –Hc), 6.53 (d, –Hd) <sup>13</sup> C NMR (DMSO): 191.46 (–CH=O), 160.99 (C5–H), 152.16 (C1- <i>ipso</i> ), 151.73 (C6- <i>ipso</i> ), 143.61 (C9- <i>ipso</i> ), 139.89 (C11,C16- <i>ipso</i> ), 132.58 (C12–H), 131.22 (C3–H), 128.84 (C8–H), 128.07 (C13–H), 126.36 (C14,C15–H,C4- <i>ipso</i> ), 120.92 (C2- <i>ipso</i> ), 116.34 (C7–H), 64.44 (C10- <i>ipso</i> )
FP-3	<sup>1</sup> H NMR (DMSO): 9.70 (s, –CH=O), 9.26 (s, –OH), 8.33 (s, –CH=N–), 7.85 (d, –Hf), 7.34 (d, –Hc), 7.27 (t, –He), 7.09 (t, –Hd), 6.76 (d, –Hb), 6.42 (d, –Ha) <sup>13</sup> C NMR (DMSO): 160.77 (C7–H), 152.71 (C3- <i>ipso</i> ), 147.30 (C8- <i>ipso</i> ), 146.67 (C11- <i>ipso</i> ), 144.36 (C2- <i>ipso</i> ), 139.75 (C13,C18- <i>ipso</i> ), 133.48 (C5- <i>ipso</i> ), 128.68 (C10–H), 127.90 (C14–H), 127.42 (C15–H), 126.35 (C16,C17–H), 124.87 (C1- <i>ipso</i> ), 123.85 (C4–H), 120.63 (C6- <i>ipso</i> ), 114.11 (C9–H), 64.04 (C12- <i>ipso</i> )

spectra have still aldehyde and amine stretch vibrations at 1690 and 3595–3659 cm<sup>−1</sup> indicating the free amine and aldehyde groups after the graft copolymerization. O–H stretch vibrations of all synthesized compounds are seen in the range of 3300–3375 cm<sup>−1</sup> as a widespread peak. Aromatic C–H and C=C vibrations are also observed between 3027 and 3058 and 1498–1600 cm<sup>−1</sup>, respectively. In addition, C–O bending vibrations are placed in the range of 1274–1285 cm<sup>−1</sup>.

<sup>1</sup>H and <sup>13</sup>C NMR analyses results of the synthesized compounds are given in Table 2. At the <sup>1</sup>H NMR spectrum of FP-1 the peaks at 12.99, 8.91, and 5.00 ppm indicate the phenolic –OH, CH=N, and –NH<sub>2</sub> protons which confirm the proposed structure. The peaks indicating the free aldehyde groups (HC=O) of the FPs are observed at 9.79 and 9.26 ppm for FP-2 and FP-3,

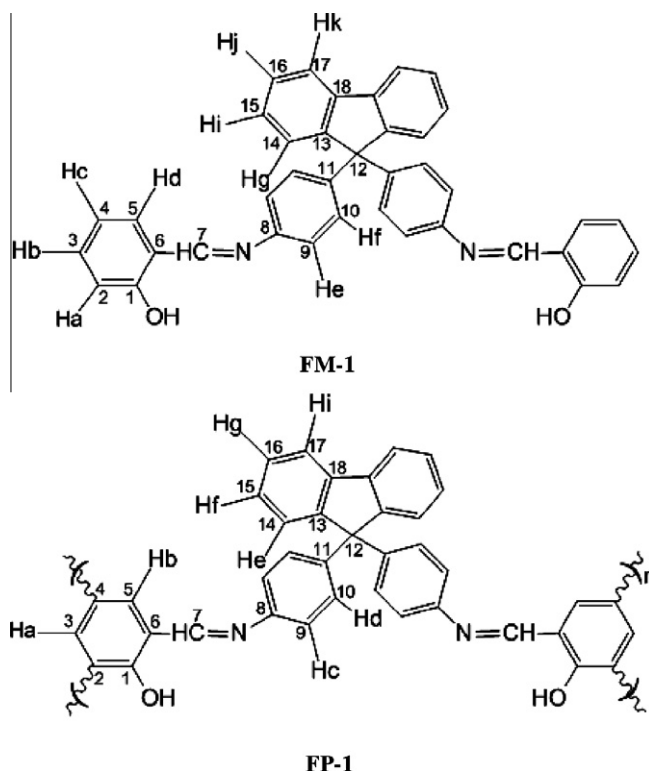


**Table 3**  
SEC analyses results of the synthesized polymers.

Compounds	Molecular weight distribution parameters																			
	Total				Fraction II				Fraction III				Fraction IV				Fraction V			
	$M_n$	$M_w$	PDI	%	$M_n$	$M_w$	PDI	%	$M_n$	$M_w$	PDI	%	$M_n$	$M_w$	PDI	%	$M_n$	$M_w$	PDI	%
FP-1 <sup>a</sup>	350	580	1.657	03	2550	4100	1.608	03	300	500	1.667	97	–	–	–	–	–	–	–	–
FP-1 <sup>b</sup>	950	1100	1.294	04	2750	3200	1.164	04	800	1000	1.250	96	–	–	–	–	–	–	–	–
FP-2 <sup>a</sup>	30,000	31,400	1.047	54	48,500	49,800	1.027	54	15,700	18,600	1.185	22	1500	1650	1.100	24	–	–	–	–
FP-2 <sup>b</sup>	37,550	38,400	1.023	58	58,000	58,700	1.012	58	15,200	18,900	1.243	21	1850	1900	1.027	21	–	–	–	–
FP-3 <sup>a</sup>	25,000	30,550	1.222	13	52,700	79,300	1.505	13	45,500	52,750	1.159	22	16,000	17,350	1.078	39	7200	8800	1.222	26
FP-3 <sup>b</sup>	28,800	35,600	1.236	21	56,200	79,250	1.410	21	46,000	52,350	1.138	21	15,900	17,600	1.107	36	7400	7500	1.014	22

<sup>a</sup> Determined by RI detector.

<sup>b</sup> Determined by UV detector.

respectively. Also, according to the <sup>13</sup>C NMR results the peaks at 175.24 and 191.46 ppm for FP-1 and FP-2, respectively, indicate the free aldehyde carbons (HC=O). Moreover, according to the <sup>13</sup>C NMR spectra chemical shift values of the coupling carbons of the FPs are higher than those of the Schiff bases due to the increasing conjugation length [22,25]. For example, in comparison of FM-1 and FP-1, after the copolymerization the peak values of C2 and C4 shift from 117.00 and 121.18 ppm to 126.24 and 133.72 ppm, respectively. Similarly, C2 peak value of FM-2 shifts from 114.22 to 120.92 ppm and C1, C2, and C5 peak values of FM-3 shift from 122.97, 116.01, and 114.62 ppm to 133.48, 123.85, and 124.87 ppm, respectively, after the copolymerization. The mentioned chemical shifts are also evidence of the polymer structures: oxidative polycondensation reaction of the phenolic com-

**Table 4**  
Electronic structure parameters of the synthesized compounds.

Compounds	<sup>a</sup> HOMO	<sup>b</sup> LUMO	<sup>c</sup> $E_g$	<sup>d</sup> $E'_g$	<sup>e</sup> $\lambda_{max}$
FM-1	–5.79	–2.75	3.14	3.04	347
FP-1	–5.40	–3.37	2.37	2.03	418
FM-2	–5.42	–2.60	3.25	2.82	327
FP-2	–5.65	–3.25	2.91	2.40	330
FM-3	–5.37	–2.94	3.21	2.43	336
FP-3	–5.39	–3.79	2.21	1.60	426

<sup>a</sup> Highest occupied molecular orbital.

<sup>b</sup> Lowest unoccupied molecular orbital.

<sup>c</sup> Optical band gap.

<sup>d</sup> Electrochemical band gap.

<sup>e</sup> Maximum absorbance wavelength.

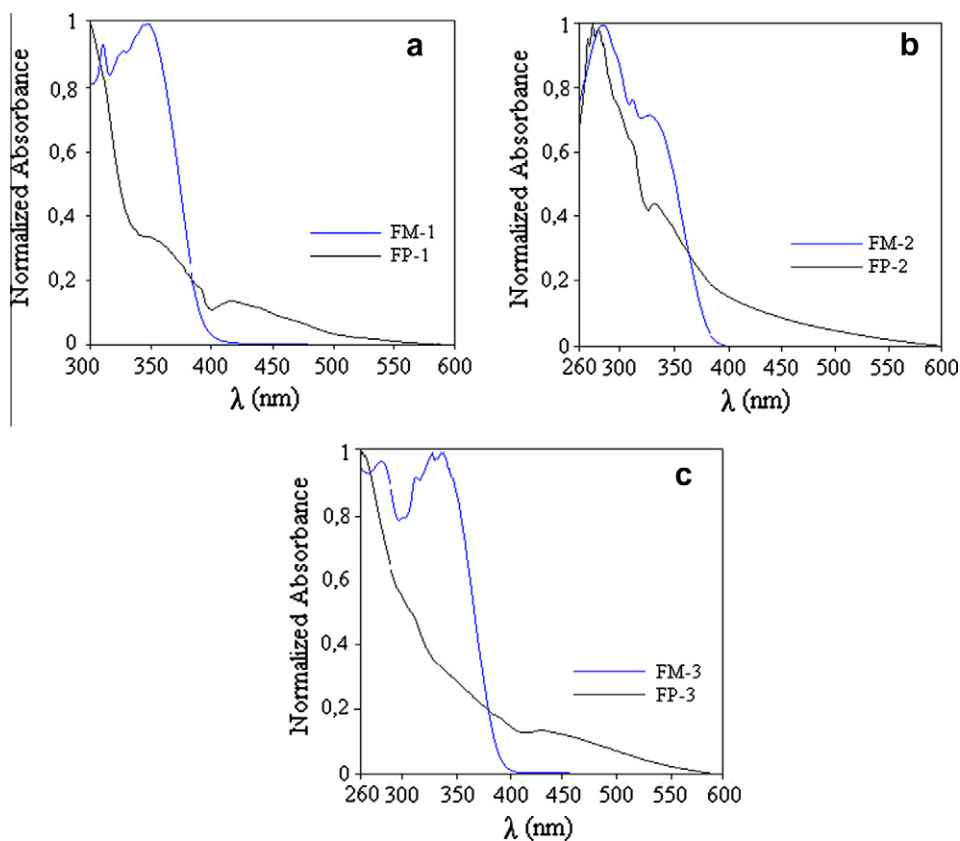


**Fig. 1.** Absorption spectra of FM-1 and FP-1 (a), FM-2 and FP-2 (b), and FM-3 and FP-3 (c).

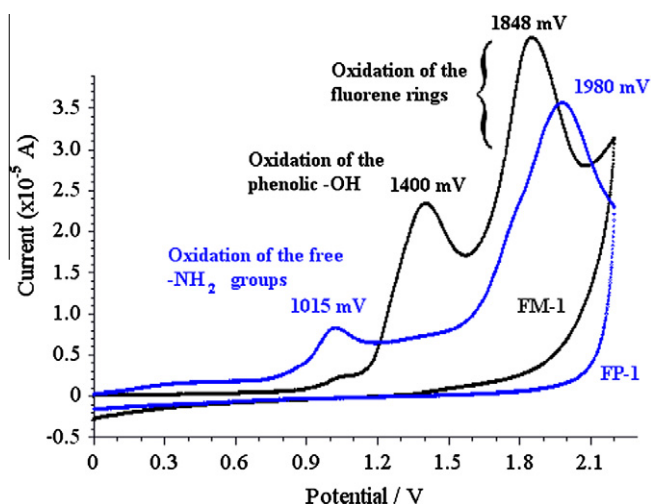


Fig. 2. Cyclic voltammograms of FM-1 and FP-1.

pounds proceeds via combination of the monomers by coupling of the phenylene (-ortho and -para positions of phenol) and oxiphenylene radicals. These combinations result in C–C and C–O–C couplings and the increasing conjugation. As a result, the coupling carbons in the polymer structures have lower electron densities and resultantly higher chemical shifts than those in their monomer compounds [23].

According to the SEC chromatograms, the calculated number-average molecular weight ( $M_n$ ), weight average molecular weight ( $M_w$ ), and polydispersity index (PDI) values of the FPs measured using both RI and UV detectors are given in Table 3. As seen in Table 3 the obtained FP-1, FP-2, and FP-3 have 2, 3, and 4 main fractions. According to the total values the molecular weight of FP-1 is lower than  $1000 \text{ g mol}^{-1}$ , whereas the total molecular weights of FP-2 and FP-3 are approximately  $30,000 \text{ g mol}^{-1}$ . These results also agree with the solubility tests. FP-1 with its low molecular weight is a fine-soluble polymer in common organic solvents and the others have lower solubilities due to their high-molecular weighted structures. Lower molecular weight of FP-1 could be attributed to mainly two factors: the first is low molecular weight of oligosalicylaldehyde used and the second is lower grafting capability of FDA onto OSA. As emphasized before the grafting of FDA onto OSA, O-4-HBA, and O-3,4-HBA is carried out by condensation reaction and new imine bonds formation. On the contrary of the others OSA has ortho –OH substituents of the aldehyde groups which may cause the steric hindrance and low grafting yield. As a result, FDA could be more easily grafted onto O-4-HBA and O-3,4-HBA due to their non-substituted structures at ortho-positions which results in higher molecular weights.

### 3.2. Optical and electrochemical properties

The UV–vis spectra of the synthesized compounds are shown in Fig. 1. According to these spectra, a red shift occurs at the absorption edges of the synthesized polymers in comparison to the Schiff bases. This is because of the polyconjugated structures of the polymers which increase HOMO and decrease LUMO energy levels thus result in lower band gaps. The optical band gaps ( $E_g$ ) could be obtained by using the following equation as in the literature [28]:

$$E_g = 1242/\lambda_{\text{onset}} \quad (1)$$

where  $\lambda_{\text{onset}}$  is the onset wavelength which can be determined by intersection of two tangents on the absorption edges.  $\lambda_{\text{onset}}$  also

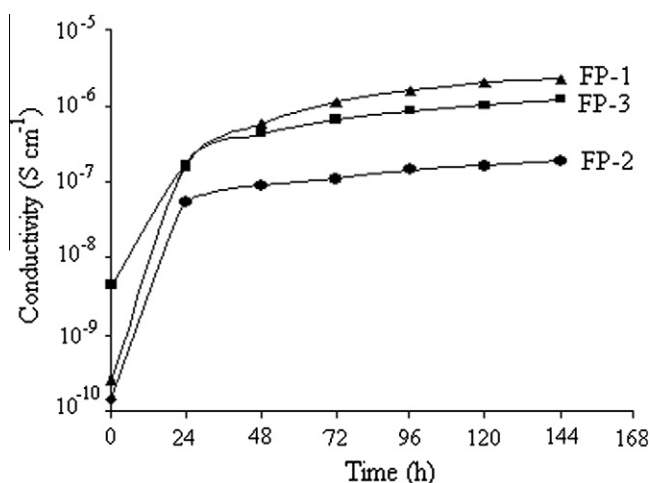


Fig. 3. Electrical conductivity changes of the  $\text{I}_2$ -doped and undoped compounds vs. doping time at  $25^\circ\text{C}$ .

indicates the electronic transition start wavelength. The calculated band gap values are given in Table 4. These results show that the synthesized polymers have lower optical band gaps when compared to the monomers, as expected.

Cyclic voltammograms of FM-1 and FP-1 are given in Fig. 2. As seen in these voltammograms both materials have two oxidation steps. At the voltammogram of FM-1 the peak at 1400 mV indicates the oxidation of the phenolic –OH group, agreed with the literature data [16]. That peak disappears at the voltammogram of FP-1 due to C–O–C coupling. Kaya et al. have previously proposed that oxidative polycondensation reaction of phenol derivatives could proceed by two mechanisms: C–C and C–O–C coupling of the monomer units [23]. Seo et al. investigated anodic oxidation pathways of aromatic amine compounds [29]. The peak at 1015 mV at the voltammogram of FP-1 indicates the oxidation of free – $\text{NH}_2$  groups, agreed with the mentioned study, while in the voltammogram of FM-1 that peak disappears, as expected. Additionally, the oxidations of the fluorene rings are seen at 1848 and 1980 mV for FM-1 and FP-1, respectively. It is known that the fluorene compounds can be oxidatively degraded at the potentials upon 1700 mV and an irreversible oxidation process is observed [30]. According to the cyclic voltammetry (CV) measurements, the HOMO–LUMO energy levels and the electrochemical band gaps ( $E_g$ ) are calculated as in the literature [31] and shown in Table 4. As seen in Table 4 the optical band gaps are a bit higher than the electrochemical band gaps. This result is in agreement with the literature [23]. However, the orders of the band gaps calculated from both optical and electrochemical data are same. According to these data the order of the fluorene co-polyphenols' band gaps is as follows:  $\text{FP-3} < \text{FP-1} < \text{FP-2}$ . Lower band gaps facilitate the electronic transitions between HOMO–LUMO energy levels and make the polymers more electro-conductive than the monomers.

### 3.3. Electrical conductivities

Electrical conductivities of the synthesized FPs and the changes of these values related to doping time with iodine are shown in Fig. 3. As well known, there is an opposite tendency between the HOMO–LUMO band gap and the conductivity. As stressed before lower band gap facilitates the electronic transition from bulk to vacuum energy level. This results in higher conductivity. FP-3 with the lowest band gap has also the highest undoped conductivity. However, the conductivity of FP-3 increases approximately two orders of magnitude whereas three and four orders for FP-2 and FP-1,

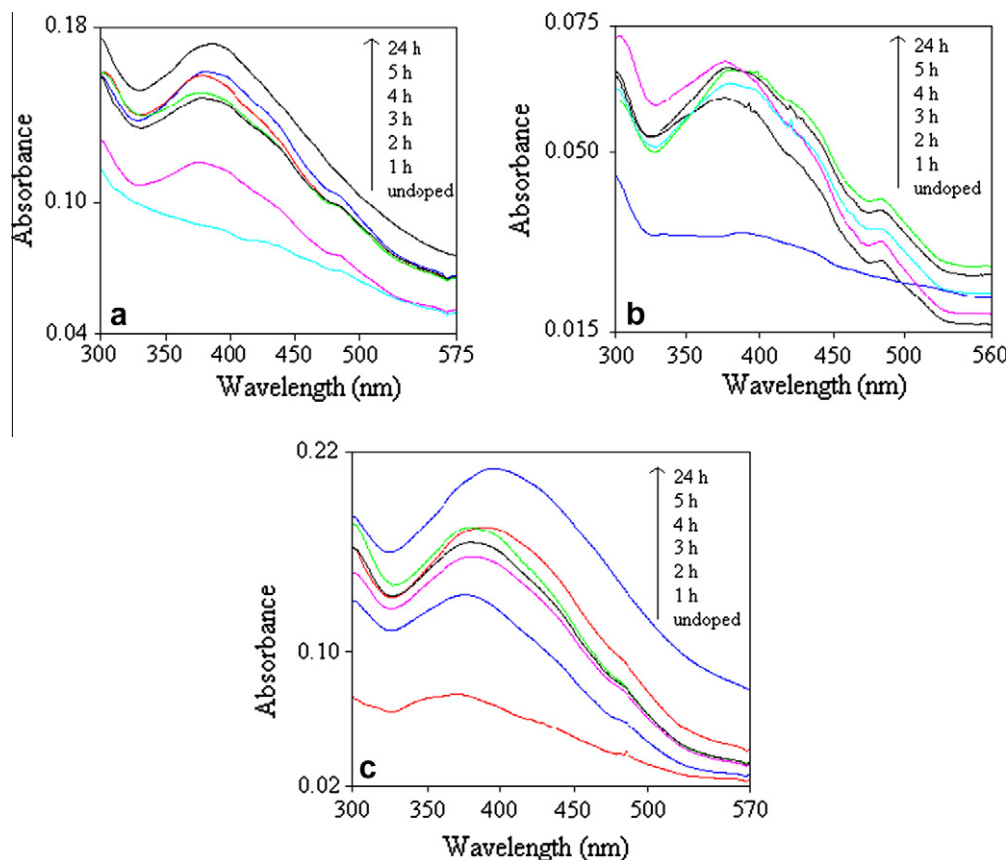


**Fig. 4.** The effect of doping procedure on the absorption spectra of the polymers: (a) the absorption spectra of doped (for between 1 and 24 h) and undoped states of FP-1, (b) FP-2, and (c) FP-3.

respectively. Maximum conductivity increasing is obtained for FP-1 via iodine doping. As a result FP-1 has the highest saturated conductivity. This is possibly because of the steric effect of the higher number of  $-OH$  substituents of FP-3 which prevent the penetrating of iodine molecule into the polymer chain. Diaz et al. suggested the doping mechanism of Schiff base polymers [32]. According to doping mechanism, nitrogen, being a very electronegative element, is capable of coordinating with an iodine molecule. As a result, a charge-transfer complex between imine compound and dopant iodine is formed and a considerable increase in conductivity can be observed [25]. However, steric hindrance of the substituents bound with the phenol ring prevents the iodine coordination and consequently could decrease the doping level of the polymer [22]. Hindson et al. synthesized triphenylamine-based poly(azomethine)s with wholly aromatic structures as the new opto-electronic materials [33]. The optical band gaps of their synthesized PAMs were found as 2.3–2.6 eV. They produced a newly photovoltaic device using the synthesized PAMs showing an external quantum efficiency (EQE) of 20% at 500 nm. The device had also an open-circuit voltage of 0.41 V and a short circuit current of  $1.23 \text{ mA cm}^{-2}$ . In another study the opto-electronic applications of some polymer charge complexes were investigated by Liu et al. [34]. They used the polymers with carbazole based side groups in device preparation. The relationship between the conductivity and polymer ratio in device was also studied. The obtained polymers were found to have potential use for low cost-printed electronics. Similarly, the presented FPs have quite low band gaps (2.20–2.90 eV) and these energy gaps become less after doping. Fluorene structure is similar to carbazol ring structure and the presented PFs including the fluorene side groups could also be useful materials in electronic or opto-electronic studies after a long time iodine doping. Conductiv-

ity measurements of imine polymers were previously studied and considerable increases were reported when they were doped with iodine [21–25,32].

The absorption spectra of the polymer films before and after doping are also given in Fig. 4. Red shifts in the absorption spectra are recorded when the polymers are exposed to iodine vapour. The growing peaks observed between 400 and 450 nm are attributed to the polaron band transitions of the imine nitrogen [35]. These new bands show that the doping procedure is successfully carried out followed by polaron formation as well as the increasing conductivity. As a result of the polaron band formation the optical band gap becomes lower which supports the increasing conductivity.

Doping procedure of conducting polymers has attracted much attention of researchers into this field, so far [36,37]. This procedure produces a lot of application fields for conducting polymers. With these properties conducting polymers are used in gas sensing materials against several kinds of electro-donor (such as  $\text{CO}$ ,  $\text{CO}_2$ ,  $\text{NH}_3$  and  $\text{H}_2\text{S}$ ) and electro-acceptor (such as  $\text{I}_2$  and  $\text{NO}_2$ ) gases [38–42]. These studies show that the doping level and electrical conductivities of a conducting polymer can be changed considerable by doping with chemical vapours. The sensing process of the conductive/semi-conductive polymers generally depends on the electron transferring mechanism from and to the analytes [42]. Electron transferring causes changes in resistance and work function ( $W_f$ ) of a conducting polymer as well as shifting of absorption edge. These kinds of polymers can be used to develop a gas sensor by measuring of the mentioned physical changes. The proposed fluorene co-polyphenols, thus, could also be used as an active layer in gas sensors for detection of electro-acceptor gases like iodine vapour by measuring of the conductivity change.

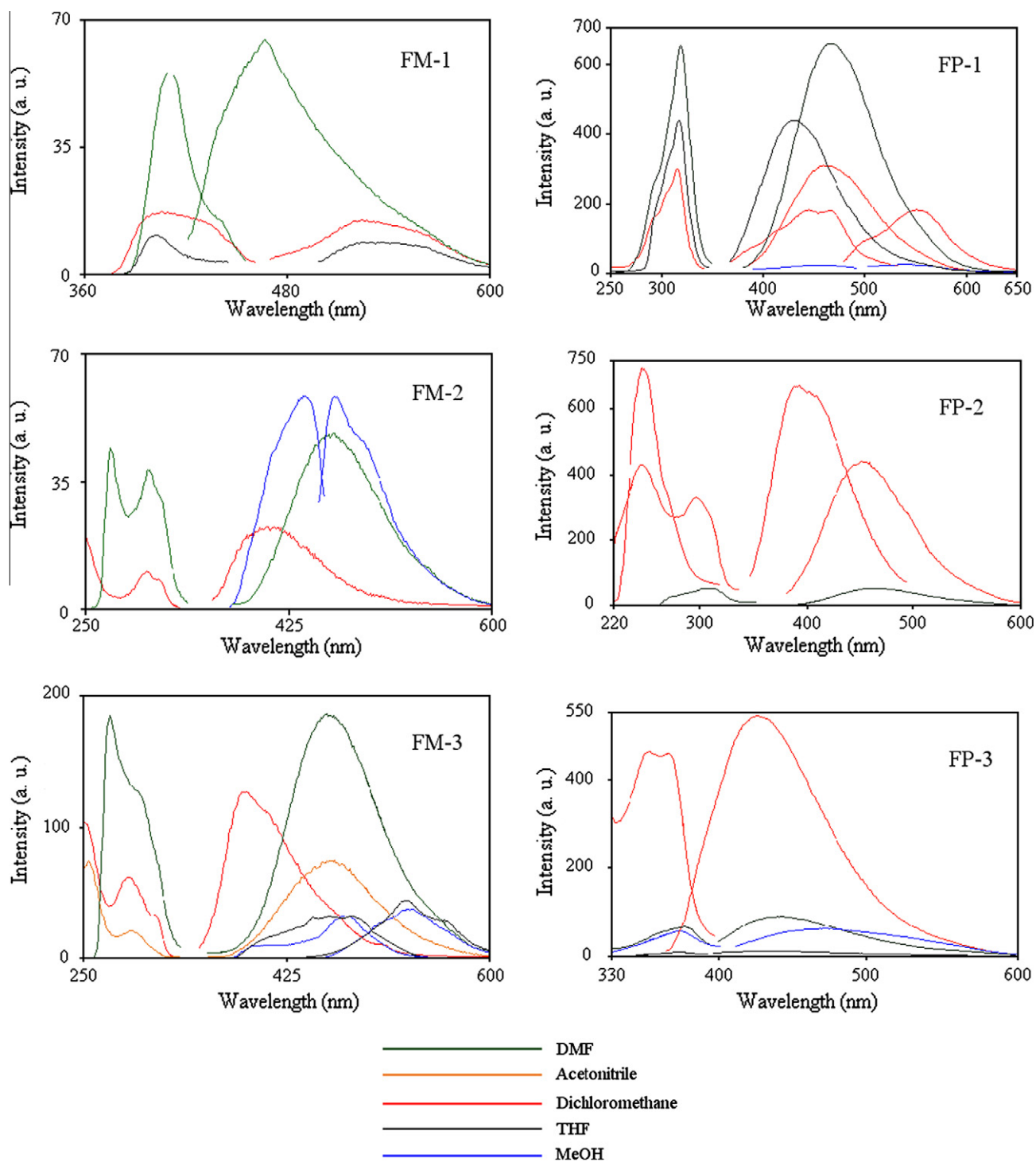


**Fig. 5.** Emission and excitation spectra of the synthesized compounds in various solvents. Conditions: slit:  $\lambda_{\text{Ex}}$  5 nm,  $\lambda_{\text{Em}}$  5 nm; concentration of the compounds: 0.01 mg/ml.

### 3.4. Fluorescence characteristics

Fluorene polymers are known as good candidates for blue emitting materials due to their unique combination of high-thermal-stability, versatile processability, and high-photoluminescence (PL) quantum yield in the solid state [43,44]. In the presented PFs fluorene unit acts as electro-donor and oligohydroxy aldehydes with the polyconjugated structures are electro-acceptors. The electron density of the fluorene ring could be transferred into the electro-acceptor oligohydroxy aldehyde chain by azomethine linkage. With UV absorption an energy transfer carries out from fluorene

ring into the oligohydroxy aldehyde chain followed by a blue emitting.

Fluorescence characteristics of the synthesized materials are determined using five separate solvents. Solvent effects on the fluorescence properties are seen in Fig. 5. It is clearly seen at the first glance into the fluorescence spectra that the synthesized FPs are highly fluorescent. On the contrary of their monomer models the quantum yields of the FPs are quite high. DMF and acetonitrile solutions of the all FPs show fine fluorescence characteristics. However, a reverse solvent effect could be observed for different FPs. For instance; at the  $\text{CH}_2\text{Cl}_2$  solution of FP-1 a

**Table 5**  
Fluorescence spectral data of the synthesized compounds in some employed solvents.

Compound	<sup>a</sup> $\lambda_{Ex}$	<sup>b</sup> $\lambda_{Em}$	<sup>c</sup> $\lambda_{max}(Ex)$	<sup>d</sup> $\lambda_{max}(Em)$	<sup>e</sup> $I_{Ex}$	<sup>f</sup> $I_{Em}$	<sup>g</sup> $\Delta\lambda_{ST}$
<sup>1</sup> FM-1	410	474	410	467	56	64	57
<sup>1</sup> FP-1	319	471	319	466	651	657	147
<sup>1</sup> FM-2	271	477	304	463	38	48	159
<sup>2</sup> FP-2	252	399	247	393	726	675	146
<sup>1</sup> FM-3	274	468	273	460	185	187	187
<sup>3</sup> FP-3	366	458	367	426	457	541	59

<sup>a</sup> Excitation wavelength for emission.

<sup>b</sup> Emission wavelength for excitation.

<sup>c</sup> Maximum emission wavelength.

<sup>d</sup> Maximum excitation wavelength.

<sup>e</sup> Maximum excitation intensity.

<sup>f</sup> Maximum emission intensity.

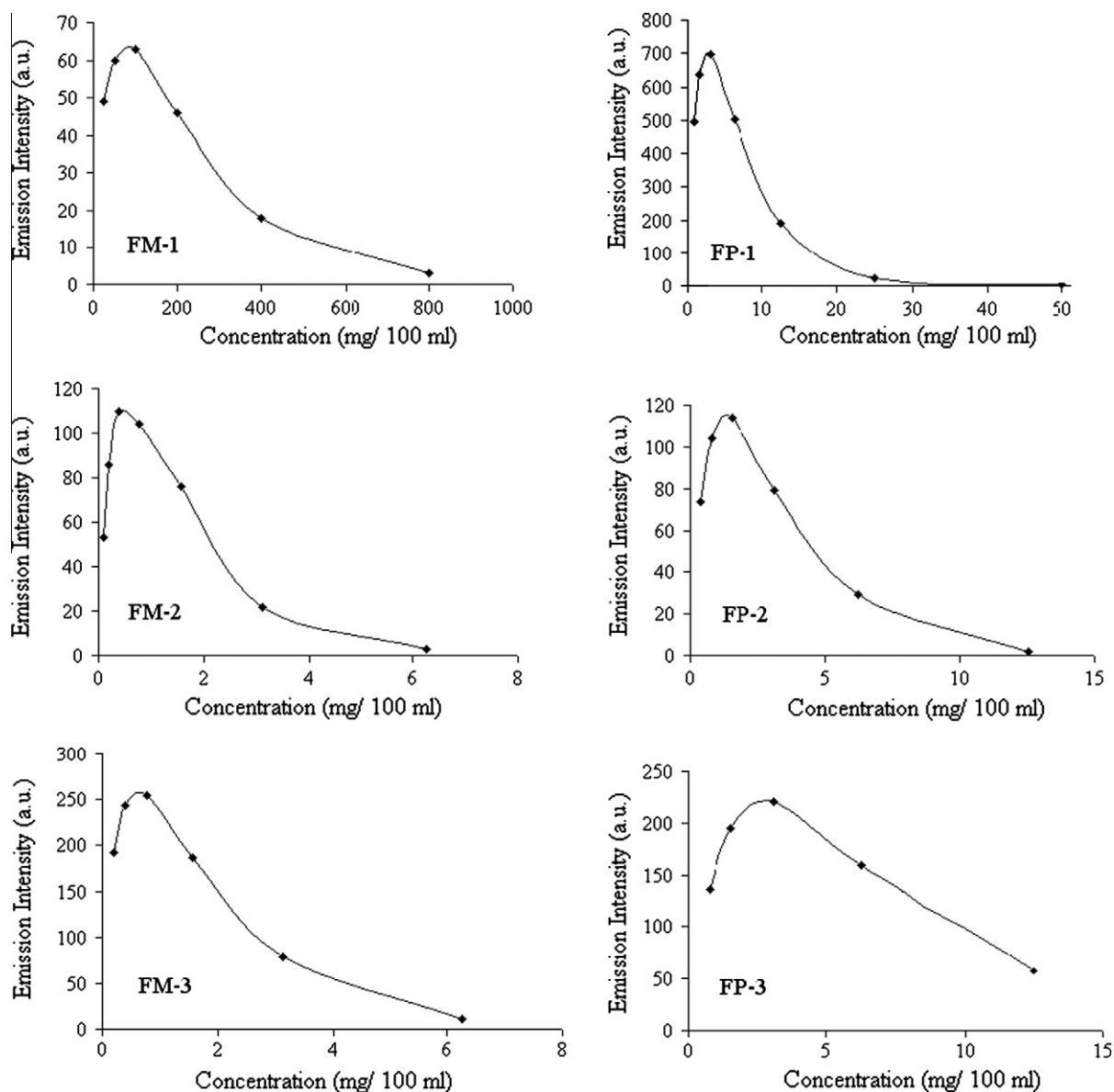
<sup>g</sup> Stoke's shift.

<sup>1</sup> DMF.

<sup>2</sup> Dichloromethane.

<sup>3</sup> Acetonitrile.

bathochromic shift is observed in comparison to the DMF solution, while for the FP-2's solutions a reverse tendency is observed. On the other hand, polarity and hydrogen bonding capacity of the solvents could influence the fluorescence properties [45].  $CH_2Cl_2$  has lower polarity than DMF and MeOH, as well as having no hydrogen bonding structure.  $CH_2Cl_2$  solutions of the synthesized compounds have generally lower emission wavelengths due to the mentioned properties (with exception of FM-1 and FP-1). Also, the emission wavelengths of methanol solutions are higher than those of the DMF solutions. This is because of the hydrogen bonding capacity of methanol. The synthesized materials have hydroxy substituents having hydrogen bonding capacity with methanol. In addition, FM-3 with its higher number of hydroxyl substituents shows higher fluorescence intensities in all solvents as well as higher red shifted spectra from  $CH_2Cl_2$  to DMF and MeOH, depending on the polarity and hydrogen bonding. However, the reverse effects of the solvents on the fluorescence spectra of

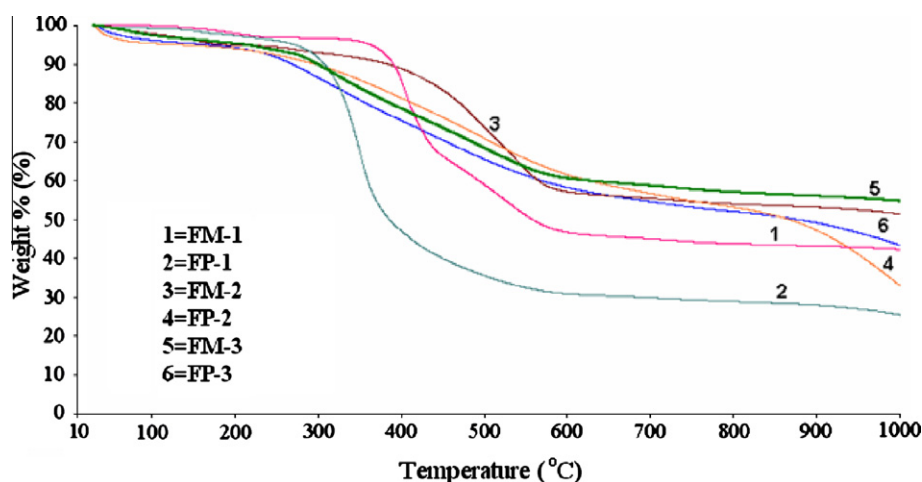


**Fig. 6.** The changes of the emission intensities of the synthesized compounds related to different concentrations. Conditions: slit:  $\lambda_{Ex}$  5 nm,  $\lambda_{Em}$  5 nm;  $\lambda_{Ex}$  410 nm and  $\lambda_{Em}$  474 nm for FM-1,  $\lambda_{Ex}$  316 nm and  $\lambda_{Em}$  469 nm for FP-1,  $\lambda_{Ex}$  271 nm and  $\lambda_{Em}$  477 nm for FM-2,  $\lambda_{Ex}$  314 nm and  $\lambda_{Em}$  468 nm for FP-2,  $\lambda_{Ex}$  255 nm and  $\lambda_{Em}$  467 nm for FM-3, and  $\lambda_{Ex}$  378 nm and  $\lambda_{Em}$  475 nm for FP-3. Solvents employed: acetonitrile for FM-3 and FP-1, and DMF for the others.

**Table 6**

Thermal degradation values of the synthesized compounds.

Compounds	<sup>a</sup> $T_{on}$	<sup>b</sup> $W_{max} \cdot T$	20% Weight losses	50% Weight losses	% Carbine residue at 1000 °C	DTA		DSC	
						Exo	Endo	<sup>c</sup> $T_g$ (°C)	<sup>d</sup> $\Delta C_p$ (J/g °C)
FM-1	379	408,525	408	561	42.28	–	229	–	–
FP-1	302	345	331	388	25.48	–	–	210	0.713
FM-2	398	529	474	–	51.33	–	253	–	–
FP-2	250	394,496	419	918	38.02	–	–	164	0.048
FM-3	253	318,489	389	–	58.27	–	–	–	–
FP-3	226	330,447	350	958	47.95	–	–	200	0.212

<sup>a</sup> The onset temperature.<sup>b</sup> Maximum weight temperature.<sup>c</sup> Glass transition temperature.<sup>d</sup> Change of specific heat during glass transition.**Fig. 7.** TGA curves of the synthesized compounds.

FM-1 and FP-1 are interesting. These materials have *o*-substituted hydroxyl groups of azomethine bond. This structure could have keto-amine  $\leftrightarrow$  phenol-imine tautomerism [46] which may cause different solvent effects on the fluorescence spectra.

Fluorescence data are also summarized in Table 5. As seen in Table 5 with exception of FM-1 and FP-3 the other synthesized materials have quite high Stoke's shift values ( $\Delta\lambda_{ST}$ ). Stoke's shift is an important value for a fluorescence sensor. The higher Stoke's shift value supplies very low background signals and resultantly allows the usage of the material in construction of a fluorescence sensor [47]. A series of Schiff bases and some chelate-structured polymer models have been presented as possible ion-selective sensors depending on quenching of the fluorescence intensity values when exposed to corresponding ion like Fe(II), Cu(II) etc. [48,49]. FP-1 and FP-3 have chelating groups as well as high fluorescence intensities and they can give a selective-sensitive response against some heavy metal ions.

The optimization of the concentrations to obtain maximal emission intensity is also investigated in different solvents (Fig. 6). The obtained results show that the synthesized materials have the maximum fluorescence intensity in the concentration range of 0.5–4 mg/100 ml (except FM-1). However, the optimum fluorescence concentration of FM-1 is quite higher than the others (32 times higher than FP-1 and FP-3; 64, 128, and 256 times higher than FP-2, FM-3, and FM-2, respectively).

### 3.5. Thermal analysis

Thermal degradation data (TGA, DTG, DTA and DSC) are summarized in Table 6. TGA curves of the synthesized compounds are also shown in Fig. 7. According to the TGA results, the initial

degradation temperatures ( $T_{on}$ ) of the polymers are lower than those of their Schiff base models. This is because of the formation of C–O etheric bond during the OP reaction (C–O–C coupling). This weak bond is easily broken at moderate temperatures and makes the polymer thermally unstable. Moreover, carbine residue values also indicate that the synthesized fluorene monomers are more thermally stable than the co-polyphenol derivatives. For example, the initial degradation temperature (°C) and carbine residue (%) are 379 and 42 for FM-1; 302 and 25 for FP-1; 398 and 51 for FM-2; 250 and 38 for FP-2; 253 and 58 for FM-3; and 226 and 48 for FP-3, respectively. With exception of FM-1 and FM-2 the DTA curves of the other materials show no clear endothermic or exothermic peaks. However, the endothermic peaks at 229 and 253 °C for FM-1 and FM-2 are recorded, respectively, indicating their melting points. According to the DSC analyses glass transition temperatures ( $T_g$ ) of the polymers are also calculated and given in Table 6. The synthesized FPs have quite high  $T_g$  values between 164 and 200 °C, agreed with the previously published Schiff base substituted oligophenol derivatives [23,25]. Also the changes of the specific heats ( $\Delta C_p$ ) during the glass transitions are calculated and the biggest change is recorded for FP-1 which followed by FP-3 and FP-2, respectively.

### 4. Conclusions

Novel fluorene Schiff bases and Schiff base substituted oligophenol derivatives containing fluorene moiety in the side chain were synthesized by condensation reaction of FDA with aromatic hydroxyaldehydes and graft copolymerization of FDA with oligohydroxyaldehydes (OSA, *O*-4-HBA, and *O*-3,4-HBA), respectively. Solubility tests showed that the synthesized compounds are fine

soluble in common organic solvents. The synthesized FPs have quite higher fluorescence intensities than their monomer models. Especially FP-1 can be a promising spectrofluorometric ion sensor because of the highly fluorescence intensity and Stoke's shift with a suitable chemical structure for complexation with metal ions. The new fluorene polymers are blue emitting materials with a good quantum yield and could be used in blue light emitting diodes preparation. According to the optical and electrochemical analyses the synthesized polymers have quite low band gaps. FP-3 has the lowest band gap and resultantly the highest undoped conductivity. The electrical conductivities of FP-1, FP-2, and FP-3 could be increased nearly 4, 2.5, and 2 orders of magnitude, respectively. According to the saturated states FP-1 had the highest conductivity. Increasing conductivity with iodine doping makes the synthesized polymers highly promising for using in gas sensing devices. Thermal degradation characteristics were also determined. Although the monomer models were found to be more stable compounds than the polymers the initial degradation temperatures of the polymers were quite high in the range of 220–300 °C. With the fine thermal stabilities they can be promising candidates for aerospace applications. Moreover, the synthesized polymers could be also used in electronic, optoelectronic, electro-active, and photovoltaic applications due to having semi-conductive structures.

#### Acknowledgement

The authors thank TÜBİTAK Grants Commission for a research grant (Project No: TBAG-107T414).

#### References

- [1] R. Tang, Z. Tan, Y. Li, F. Xi, *Chem. Mater.* 18 (2006) 1053.
- [2] A. Donat-Bouillud, *Chem. Mater.* 12 (2000) 1931.
- [3] M. Leclerc, *J. Polym. Sci. Part A: Polym. Chem.* 39 (2001) 2867.
- [4] M. Francisco, M. Ricardo, *Adv. Funct. Mater.* 17 (2007) 71.
- [5] M. Fukuda, K. Sawada, S. Morita, K. Yoshino, *Synthetic Met.* 41 (1991) 855.
- [6] Z. Caimao, C. Zhiyuan, B. Weibin, Y. Xi, *Wuhan Univers. J. Nat. Sci.* 12 (2007) 327.
- [7] B. Dong, D. Song, L. Zheng, J. Xu, N. Li, *J. Electroanal. Chem.* 633 (2009) 63.
- [8] D. Marsitzky, J. Murray, J.C. Scott, K.R. Carter, *Chem. Mater.* 13 (2001) 4285.
- [9] M. Fukuda, K. Sawada, K. Yoshino, *J. Polym. Sci. Polym. Chem. Ed.* 31 (1993) 2465.
- [10] Q. Pei, Y. Yang, *J. Am. Chem. Soc.* 118 (1996) 7416.
- [11] S. Kappaun, M. Zelzer, K. Bartl, R. Saf, F. Stelzer, C. Slugovc, *J. Polym. Sci. Polym. Chem. Ed* 44 (2006) 2130.
- [12] H.C. Kim, J.S. Kim, K.S. Kim, H.K. Park, S. Baek, M. Ree, *J. Polym. Sci. Part A: Polym. Chem.* 42 (2004) 825.
- [13] M. Bruma, E. Hamciuc, B. Schulz, T. Kopnick, Y. Kaminorz, J. Robison, *Macromol. Symp.* 199 (2003) 511.
- [14] M.H. Shin, J.W. Huang, M.C. Huang, C.C. Kang, W.C. Chen, M.Y. Yeh, *Polym. Bull.* 60 (2008) 597.
- [15] S. Destri, M. Pasini, C. Pelizzi, W. Porzio, G. Predieri, C. Vignali, *Macromolecules* 32 (1999) 353.
- [16] F.C. Tsai, C.C. Chang, C.L. Liu, W.C. Chen, S.A. Jenekhe, *Macromolecules* 38 (2005) 1958.
- [17] İ. Kaya, M. Yıldırım, *Eur. Polym. J.* 43 (2007) 127.
- [18] İ. Kaya, A.R. Vilayetoğlu, H. Mart, *Polymer* 42 (2001) 4859.
- [19] İ. Kaya, A. Bilici, *J. Appl. Polym. Sci.* 104 (2007) 3417.
- [20] İ. Kaya, H.Ö. Demir, A.R. Vilayetoğlu, *Synthetic Met.* 126 (2002) 183.
- [21] İ. Kaya, A. Bilici, *Polimery* 52 (2007) 827.
- [22] İ. Kaya, M. Yıldırım, *J. Appl. Polym. Sci.* 110 (2008) 539.
- [23] İ. Kaya, M. Yıldırım, M. Kamacı, *Eur. Polym. J.* 45 (2009) 1586.
- [24] A. Iwan, D. Sek, *Prog. Polym. Sci.* 33 (2008) 289.
- [25] İ. Kaya, M. Yıldırım, *Synthetic Met.* 159 (2009) 1572.
- [26] H. Mart, H. Yürük, M. Saçak, V. Muradoğlu, A.R. Vilayetoğlu, *Polym. Degrad. Stabil.* 83 (2004) 395.
- [27] M.K. Ram, M. Joshi, R. Mehrotra, S.K. Dhawan, S. Chandra, *Thin Solid Films* 304 (1997) 65.
- [28] K. Colladet, M. Nicolas, L. Goris, L. Lutsen, D. Vanderzande, *Thin Solid Films* 451 (2004) 7.
- [29] E.T. Seo, R.F. Nelson, J.M. Fritsh, L.S. Marcoux, D.W. Leedy, R.N. Adams, *J. Am. Chem. Soc.* 88 (1966) 3498.
- [30] F. Montilla, R. Mallavia, *Adv. Funct. Mater.* 17 (2007) 71.
- [31] R. Cervini, X.C. Li, G.W.C. Spencer, A.B. Holmes, S.C. Moratti, R.H. Friend, *Synthetic Met.* 84 (1997) 359.
- [32] F.R. Diaz, J. Moreno, L.H. Tagle, G.A. East, D. Radic, *Synthetic Met.* 100 (1999) 187.
- [33] J.C. Hindson, B. Ulgut, R.H. Friend, N.C. Greenham, B. Norder, A. Kotlewski, T.J. Dingemans, *J. Mater. Chem.* 20 (2010) 937.
- [34] S. Liu, J. Shi, E.W. Forsythe, S.M. Blomquist, D. Chiu, *Synthetic Met.* 159 (2009) 1438.
- [35] S.-A. Chen, G.-W. Hwang, *Macromolecules* 29 (1996) 3950.
- [36] K.H. Lee, J. Ohshita, A. Kunai, *Organometallics* 23 (2004) 5365.
- [37] A.G. MacDiarmid, *Synthetic Met.* 125 (2001) 11.
- [38] B. Adhikari, S. Majumdar, *Prog. Polym. Sci.* 29 (2004) 699.
- [39] N.E. Agbor, M.C. Petty, A.P. Monkman, *Sens. Actuat. B* 28 (1995) 173.
- [40] R.D. McCullough, *Adv. Mater.* 10 (1998) 93.
- [41] L. Ruangchuay, A. Sirivat, J. Schwank, *React. Funct. Polym.* 61 (2004) 11.
- [42] H. Bai, G.Q. Shi, *Sensors* 7 (2007) 267.
- [43] A. Babel, S.A. Jenekhe, *Macromolecules* 36 (2003) 7759.
- [44] K. Takagi, H. Kakiuchi, Y. Yuki, M. Suzuki, *J. Polym. Sci. Part A: Polym. Chem.* 45 (2007) 4786.
- [45] J.R. Lakowicz, *Principles of Fluorescence Spectroscopy*, 3rd printing, Plenum Press, New York, 1986.
- [46] İ. Kaya, M. Yıldırım, A. Avci, *Synthetic Met.* 160 (2010) 911.
- [47] O. Oter, K. Ertekin, R. Kılınçarslan, M. Ulusoy, B. Çetinkaya, *Dyes Pigments* 74 (2007) 730.
- [48] S. Derinkuyu, K. Ertekin, O. Oter, S. Denizaltı, E. Çetinkaya, *Anal. Chim. Acta* 588 (2007) 42.
- [49] N. Aksuner, E. Henden, İ. Yılmaz, A. Çukurovalı, *Sens. Actuat. B* 134 (2008) 510.